REPORT DOCUMENTATION PAGE

Form Approved OMB NO. 0704-0188

1. REPORT DATE (DD-MM-YYYY)	2. REPORT TYPE	3. DATES COVERED (From - To)
21-05-2012	Final Report	1-May-2007 - 31-Dec-2011

4. TITLE AND SUBTITLE

FINAL REPORT: Magneto-Transpots in interband Resonant Tunneling Diodes (I-RTDs) and Dilute Magnetic Semiconductor (DMS) I-RTDs

5a. CONTRACT NUMBER

5b. GRANT NUMBER
W911NF-04-D-0003

5c. PROGRAM ELEMENT NUMBER
611102

6. AUTHORS
Dwight Woolard, Weidong Zhang

5d. PROJECT NUMBER

5e. TASK NUMBER

5f. WORK UNIT NUMBER

7. PERFORMING ORGANIZATION NAMES AND ADDRESSES

North Carolina State University
Office of Contract and Grants
Leazar Hall Lower Level- MC
Raleigh, NC 27695 -7214

8. PERFORMING ORGANIZATION REPORT NUMBER

9. SPONSORING/MONITORING AGENCY NAME(S) AND ADDRESS(ES)

U.S. Army Research Office
P.O. Box 12211
Research Triangle Park, NC 27709-2211

10. SPONSOR/MONITOR'S ACRONYM(S)
ARO

11. SPONSOR/MONITOR'S REPORT NUMBER(S)
52918-EL-SR.4

12. DISTRIBUTION AVAILIBILITY STATEMENT

Approved for Public Release; Distribution Unlimited

13. SUPPLEMENTARY NOTES

The views, opinions and/or findings contained in this report are those of the author(s) and should not contrued as an official Department of the Army position, policy or decision, unless so designated by other documentation.

14. ABSTRACT

This final report discusses a completely novel approach for generating THz frequency radiation that utilizes "interband" transitions and tunneling processes which can be induced simultaneously within double-barrier (DB) GaSb/InAs/GaSb broken-gap (BG) resonant-tunneling-diodes (RTDs). This DB-BG-RTD device will utilizes two distinct innovations. First, ultra-fast heavy-hole (HH) interband tunneling is leveraged to depopulate a lower, valence-band (VB) well-state E1 which then allows electrons resonantly injected into an upper conduction-band

15. SUBJECT TERMS

InAs, GaSb, Terahertz, lasing, interband tunneling

16. SECURITY CLASSIFICATION OF:			17. LIMITATION OF ABSTRACT	15. NUMBER OF PAGES	19a. NAME OF RESPONSIBLE PERSON
a. REPORT	b. ABSTRACT	c. THIS PAGE			Dwight Woolard
UU	UU	UU	UU		19b. TELEPHONE NUMBER: 919-549-4297

Report Title

FINAL REPORT: Magneto-Transpots in interband Resonant Tunneling Diodes (I-RTDs) and Dilute Magnetic Semiconductor (DMS) I-RTDs

ABSTRACT

This final report discusses a completely novel approach for generating THz frequency radiation that utilizes "interband" transitions and tunneling processes which can be induced simultaneously within double-barrier (DB) GaSb/InAs/GaSb broken-gap (BG) resonant-tunneling-diodes (RTDs). This DB-BG-RTD device will utilizes two distinct innovations. First, ultra-fast heavy-hole (HH) interband tunneling is leveraged to depopulate a lower, valence-band (VB) well-state E1 which then allows electrons resonantly injected into an upper conduction-band (CB) well-state E2 (i.e., center region of the RTD) to serve as the electron source for the light-generating recombination at small photonic energy differences E2 - E1 lying within the THz regime. Second, the associated electrons and holes pairs are spatially-delocalized (SD) by the RTD heterostructures which leads to a significant suppression of all degrading nonradiative recombination processes. These effects allow for large population inversions and optical gains that may be used in single DB-BG-RTD microdisk laser structures operating at near room temperature (~ 280 K) to produce 1-10 mW in the 1-3 THz gap region, which is a substantial improvement to the existing state-of-the-art solid-state THz source technology (i.e., < 0.1 mW). Furthermore, it is expected that novel quantum-dot DB-BG-RTD nanopillar-array architectures can be used to further reduce drive-current heating effects to achieve additional multiplication of the output power.

Enter List of papers submitted or published that acknowledge ARO support from the start of the project to the date of this printing. List the papers, including journal references, in the following categories:

(a) Papers published in peer-reviewed journals (N/A for none)

Received	Paper

TOTAL:

Number of Papers published in peer-reviewed journals:

(b) Papers published in non-peer-reviewed journals (N/A for none)

Received	Paper

TOTAL:

Number of Papers published in non peer-reviewed journals:

(c) Presentations

Dwight Woolard and Weidong Zhang, "THz Lasing Concepts Based upon InAs/GaSb Broken-Gap Heterostructures", International Forum on Terahertz Sepectroscopy and Imaging, Kaiserrslautern, Germany, March 2, 2010.

Weidong Zhang and Dwight Woolard, "Optical gain in broken-gap nanocrystal arrays for verylong wavelength lasing applications", ISSSR Conference, Springfield, MO, June 23, 2010.

Dwight Woolard and Weidong Zhang, " THz Lasing Concepts Based Upon InAs/GaSb Broken-Gap Heterostructures," Photonics West 2011, Terahertz Technology and Applications IV, San Francisco, CA, January 22-27, 2011 (invited talk).

Weidong Zhang and Dwight Woolard, "An Assessment of Long-Wavelength Optical-Gain in Broken-Gap Heterostrucres and Quantum Dot Arrays," the International Workshop on Optical Terahertz Science and Technology, Santa Barbara, CA, March 13-17, 2011 (poster presentation).

Number of Presentations: 4.00

Non Peer-Reviewed Conference Proceeding publications (other than abstracts):

Received	Paper

TOTAL:

Number of Non Peer-Reviewed Conference Proceeding publications (other than abstracts):

Peer-Reviewed Conference Proceeding publications (other than abstracts):

Received	Paper

TOTAL:

Number of Peer-Reviewed Conference Proceeding publications (other than abstracts):

(d) Manuscripts

Received	Paper

TOTAL:

Number of Manuscripts:

Books

Received	Paper

TOTAL:

Patents Submitted

Patents Awarded

Awards

Graduate Students

NAME	PERCENT_SUPPORTED

FTE Equivalent:

Total Number:

Names of Post Doctorates

NAME	PERCENT_SUPPORTED

FTE Equivalent:
Total Number:

Names of Faculty Supported

NAME	PERCENT_SUPPORTED

FTE Equivalent:
Total Number:

Names of Under Graduate students supported

NAME	PERCENT_SUPPORTED

FTE Equivalent:
Total Number:

Student Metrics

This section only applies to graduating undergraduates supported by this agreement in this reporting period

The number of undergraduates funded by this agreement who graduated during this period:	0.00
The number of undergraduates funded by this agreement who graduated during this period with a degree in science, mathematics, engineering, or technology fields:.....	0.00
The number of undergraduates funded by your agreement who graduated during this period and will continue to pursue a graduate or Ph.D. degree in science, mathematics, engineering, or technology fields:.....	0.00
Number of graduating undergraduates who achieved a 3.5 GPA to 4.0 (4.0 max scale):	0.00
Number of graduating undergraduates funded by a DoD funded Center of Excellence grant for Education, Research and Engineering:	0.00
The number of undergraduates funded by your agreement who graduated during this period and intend to work for the Department of Defense	0.00
The number of undergraduates funded by your agreement who graduated during this period and will receive scholarships or fellowships for further studies in science, mathematics, engineering or technology fields:	0.00

Names of Personnel receiving masters degrees

NAME

Total Number:

Names of personnel receiving PHDs

NAME

Total Number:

Names of other research staff

NAME	PERCENT_SUPPORTED

FTE Equivalent:
Total Number:

Sub Contractors (DD882)

Inventions (DD882)

Scientific Progress

Please refer to the attachment for a discussion of:

I The InAs-GaSb THz lasing concept
II InAs/GaSb Broken-Gap Quantum Dot Arrays
III The InAs/GaSb Quantum Pillars
IV The Training of THz Electronics and Spectroscopy by Physical Domains
V Experimental Setups for Testing InAs-GaSb THz Lasing Concept
VI Modeling and Simulations of Conduction in Molecular Systems
VII Publications and Presentations in 2010-March, 2011

Technology Transfer

FINAL REPORT

Magneto-Transpots in interband Resonant Tunneling Diodes (I-RTDs) and Dilute Magnetic Semiconductor (DMS) I-RTDs

Contents

Authored by

Weidong Zhang

Department of ECE, North Carolina State University, Raleigh, NC, 27695

Dwight Woolard

U.S. Army Research Offices, RTP, NC 27709, USA

Date: 3/02/2011

I. The InAs-GaSb THz lasing concept

The advantageous property of broken-gap InAs/GaSb heterostructure from the 6.1 Å family is that the valence band bottom of GaSb is 0.15 eV above the conduction band bottom of InAs. Hence within the adjacent InAs conduction-band (CB) well and the GaSb heavy-hole (HH) valence-band (VB) well systems, the individual electron and hole energy-levels may be positioned close enough to allow for very long wavelength recombination though the same time the overlaps of individually quantum confined wave functions are small.

In this part of investigations, we explore a novel approach for the generation of THz radiation that utilizes "interband" transitions and tunneling processes occurring simultaneously within double-barrier GaSb/InAs/GaSb broken gap structures.

The key innovations are the use of heavy-hole (HH) interband tunneling to realize ultra-fast depopulation of the lower state, and interband optical recombination while certain nonradiative processes(e.g. phonon and Auger) are suppressed. The basic approach is illustrated in Fig. 1 (a). The double-barrier GaSb/InAs/GaSb is sandwiched between two n highly doped InAs contacts. The GaSb layers present potential barriers for electrons and wells for holes. At an appropriate forward bias, two processes contribute to the transport. The first is conduction band (CB) resonant tunneling where electrons transverse the energy level E_2 inside the double barriers. The second is interband tunneling of electrons from the quasi-bound HH level E_1 within the right valence band (VB) well into the unfilled states of the collector. As a result of the depopulation of VB electrons, heavy holes are created within the right VB well. The spatial heavy hole charge accumulation in this region is maintained when the heavy-hole interband tunneling prevails over the filling up from nonradiative scattering of electrons from the CB resonant level. The injected CB electrons are able to recombine with the trapped holes to produce photonic emission with energy E_2-E_1 since the resonant CB wavefunction significantly penetrates through the right barrier and propagates into the spacer/collector. The very long-wavelength emission is a result of the large broken gap (i.e. the valance band top of GaSb is 0.15 eV above the conduction band bottom of InAs). This broken-gap alignment, which does not present any potential-energy barrier to interband tunneling, also produces rapid population inversion.

The estimation of time constant (τ_1) of heavy hole tunneling is plotted in Fig. 1 (b). This calculation has already taken into account that conduction electrons could be injected into the HH well through interband tunneling from left side emitter when the broadening of energy level E_2 is overlapped with level E_1. The fact that τ_1 is extremely short less than 1 ps at large in-plane momentum k_t is very remarkable. τ_1 is in the order of 30ps at some momentum k_t <0.01/nm. For comparison, relevant time constants as a function of k_t are studied. These typical results show that the photonic recombination time τ_{sp} is in the order of 10-100 ns, the acoustic phonon scattering time τ_{ap} is in the order of μs, and the polar optical phonon (POP) mode scattering time τ_{op} is in the order of 800 ps and the Auger recombination time is in the order of ns. These relaxation time constants are greater than heavy-hole tunneling time τ_1. Hence the interband tunneling of depopulation is rapid enough to help establish population inversion. The ultrafast interband depopulation and the suppression of nonradiative processes allow InAs/GaSb I-RTD Laser diodes potentially to operate at high temperatures. Moreover, our calculation also shows significant optical gain ~1000/cm for the wavelength range beyond 20 μm may be obtained (Fig. 1 (c)).

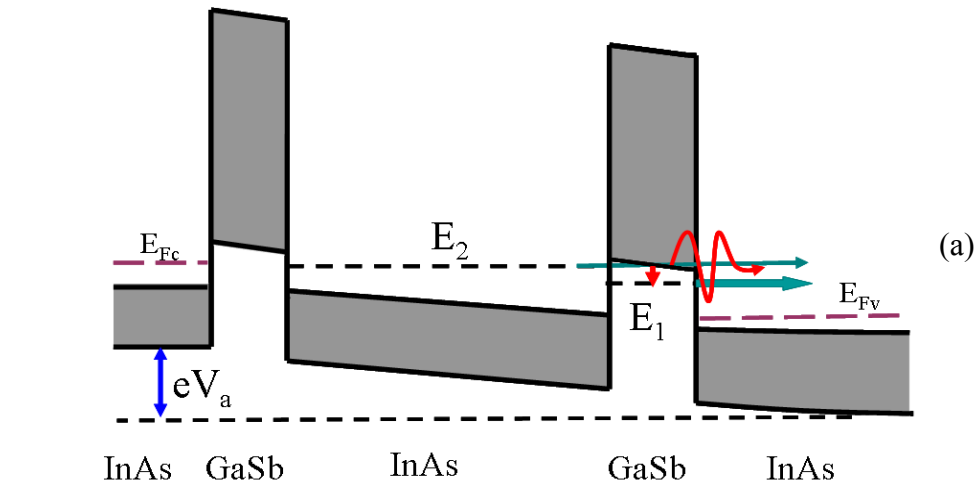

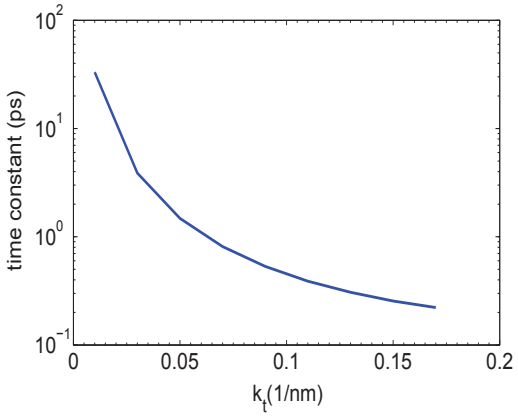

(b)

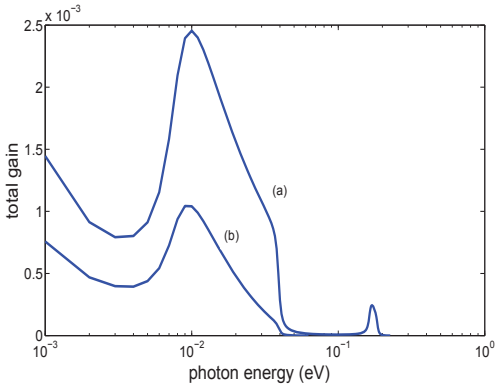

(c)

Figure 1 (a)The concept of broken-gap heterostructure lasing. E_2 is the CB level; E_1 is the HH level. The upper horizontal arrow represents the CB resonant tunneling; The lower horizontal arrow represents the HH interband tunneling. $E_{Fc,(v)}$ is the Fermi level at the emitter (collector). (b) The time constant for HH interband tunneling. The structure parameters used in calculations are: the widths of left barrier b_1=2.0 nm, right barrier b_2=5.0 nm, CB well w=11.4 nm , and the doping density in collector region $N_{dR}=7.4\times10^{17}/cm^3$. (c) The total optical gain versus photon energy at different doping density in emitter (a) $3\times10^{18}/cm^3$, (b) $2\times10^{17}/cm^3$. Optical gain=total gain per unit length; the active length ~10nm.

II. InAs/GaSb Broken-Gap Quantum Dot Arrays

In this part of research we look into three dimensional confined InAs/GaSb quantum dots, in which the competitions from non-radiative processes may be further restrained. The energy levels are truly discretized in quantum dots. As long as the photonic energy isn't fallen into optical phonon energy range (i. e. tens of eV), the phonon relaxation is a slow process. As will be shown, the spatial separation of electron-hole pairs may actually be turned into an advantage.

We study is a hypothetically simplified device structure in Fig. 2 (a). The inner InAs region is approximated as a sphere surrounded by the outer GaSb shell. The device concept in a three-level system is illustrated by Fig. 2 (b). Under optical pumping, an electron-hole pair is generated on the ground conduction band level E_2 and valence band level E_0. Then the heavy hole relaxes from energy level E_0 to the ground state E_1. The heavy hole's relaxation is fast through the intersubband Auger recombination since a few valence band electrons are populated in E_1. The stimulated emission occurs between ground levels E_2 and E_1. The energy levels E_2, E_1 may be close enough to each other for long-wavelength optical recombination relying on the sizes of quantum dots. The pumping light is circularly polarized so that the interband transition E_0 to E_2 is allowed and the intraband transition E_0 to E_1 is forbidden. Moreover, electron and hole located in different shells are distanced from each other and can't be compensated because of the special band-edge alignments. Therefore extra energy is required to put another electron-hole pair into InAs inner sphere and GaSb outer shell in order to overcome uncompensated Coulomb interaction as illustrated in Fig.2(c). The resulting "non-negligible Stark shift" in broken-gap quantum dot allows stimulated transition to win over photon's absorption (Fig. 2 (d)). It is expected that optical gain is available through the single-exciton pumping. Therefore the multiple-exciton pumping is avoided in which harmful Auger recombination usually becomes significant. The advantage of single-exciton lasing concept was proved in Cds/ZnSe nanocrystal quantum dots with Type II heterostructure by Klimov. Another advantage of the laser concept is the quantum dots are undoped. Hence the loss from strong free electron absorption in THz spectrum can be prevented.

The modeling and computing is based upon multiband Kane formulism in the spherical representation. The calculations show the excition-excition interaction energy could be ~13meV that is in the same order of inhomogeneous linewidth originating from the reasonable ~10% size variation of quantum dots. Thus the average number of exciton per site is ~0.76, right between the threshold 2/3 and the maximum 1. Hence the single-exciton stimulated emission is possible in this design. The Auger recombination resulting from multi-exciton pumping can be suppressed. The excition energy is accessible to the THz spectrum in the pseudo InAs/GaSb "atom" with proper inner spherical and outer shell radius (Fig. 2 (e)). The estimation on the maximum optical gain is plotted in Fig.2 (f) suggesting decent THz gain can be obtained from an array of InAs/GaSb quantum dots.

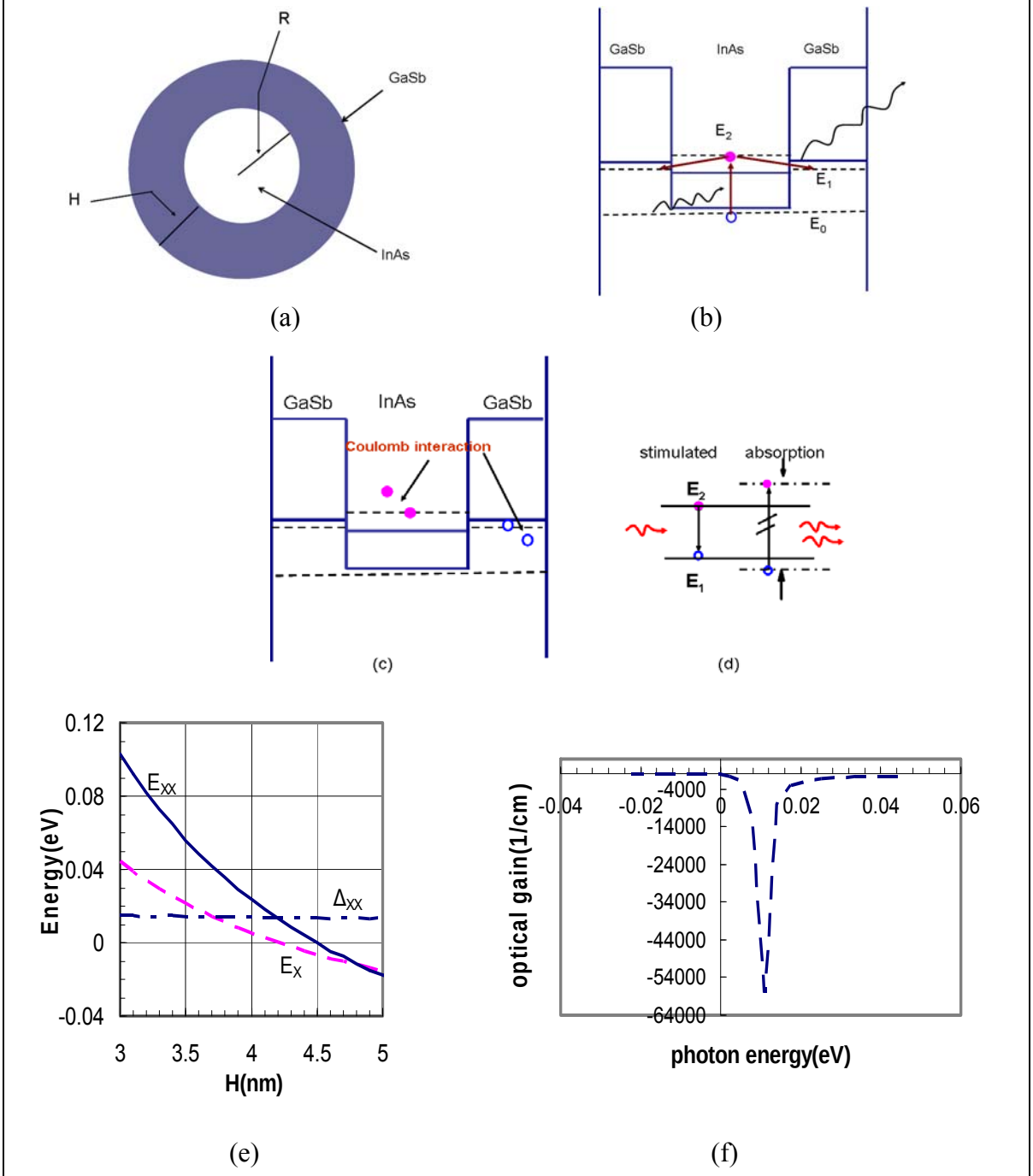

Figure 2 (a) The spherical approximation. (b) The three-energy level electron transitions. (c) The Coulomb interactions arising in the generation of biexciton in broken-gap quantum dot, and (d) the stimulated emission verse stimulated absorption. (e) The single and bi-exciton energies at R 9nm. (f) The maximum optical gain at 9nm.

III. The InAs/GaSb Quantum Pillar

According to literatures, type II superlattice pillars fabricated using electron beam lithography can achieve the diameter as small as 20nm.

We extend our studies on the InAs/GaSb quantum pillars for THz lasing. The structure of multiple InAs/GaSb pillars is shown in Fig. 3 (a), (b). As the lateral dimension of individual pillar is confined in tens of nanometers, the available in-plane momentum (x-y plane) k_t is effectively quantized. This quantization will have the CB injected current (which is the summarization of transmissions over k_t) significantly reduced and the optical phonon scattering further constrained (Fig. 3 (c).) Meanwhile, the HH interband tunneling at discretized k_t remains ultrafast and significant optical gain can still be accomplished (Fig. 3(d)). Furthermore, the TE polarization of interband radiation allows the implementation of the surface emission in a large area.

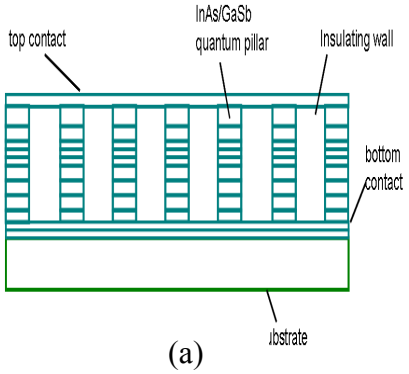

(a)

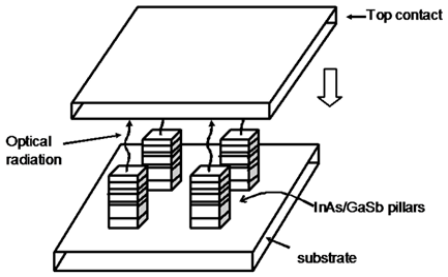

(b)

time constant for base mode, k_t=0.061	
HH tunneling	0.5ps
Auger	189ps
Optical Phonon	~941ps
Acoustic Phonon	~13.5ns
Optical Recombination	1.0ns

(c)

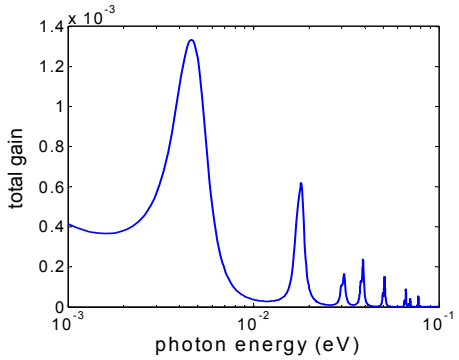

(d)

Figure 3 (a), (b) Quantum dot array for surface emission. (c) The total gain Well width 13nm, left barrier 2nm, right barrier width 5 nm, Fermi level in emitter of 0.0478eV, Fermi level in collector of 0.0173eV , doping $2\times10^{17}/cm^3$. (d) Time constants. (d) Optical gain.

IV. The Training THz electronics and spectroscopy by Physical Domains

The training was given by Physical Domains LLC, is a small business leading in developments of THz devices and techniques. This "hand on" training will help prepare Dr. Zhang for setting up and executing future experiments on novel nanoscale interband resonant tunneling diode or other THz devices in support of the existing NCSU/ARO project.

The training programs include the following activities:

(1) Measurement of coherent-power responsivity of LiTaO3 pyroelectric detector with integrated transimpedance amplifier (TIA) using two "spot" measurements at 0.104 THz (InP Gunn oscillator) and 0.530 THz (VDI FEM module).
(2) Measurement of electrical noise of LiTaO3 pyroelectric detector + TIA using a digital lock-in amplifier (SRS-810).
(3) Calculation of the noise-equivalent power (NEP) of the pyroelectric detector at 0.104 and 0.53 THz using the results of (1) and (2) above.
(4) Measurement of thermal radiation responsivity of LiTaO3 pyroelectric detector using a THz "grey" body at two separate temperatures. The "grey" body of choice will be warm water in a polyethylene bottle, which is known to produce an emissivity of approximately 0.8 across the lower-THz region.
(5) Calculation of the noise-equivalent temperature difference (NETD) of the pyroelectric detector using the results of (4) and (2).
(6) Measurement of the current-voltage characteristic of a THz zero-bias Schottky diode (ZBD).
(7) Measurement of the noise voltage from ZBD using ultra-low-noise operational amplifier.
(8) Measurement of thermal radiation responsivity of ZBD using the same "grey" body as in (4)
(9) Calculation of the NETD for the ZBD using (7) and (8).
(10) Measurement of THz power from PD photoconductive switch using calibrated pyroelectric detector.
(11) Assembly of THz simultaneous transmit/receiver T/R module.
(12) Measurement of THz frequency from FEM coherent source using THz T/R module acting as a Mach-Zender interferometer.
(13) Operation of commercial coherent photomixing transceiver (PB7100).
(14) THz spectral characterization of canonical samples from the three states of matter: (i) water vapor in the ambient environment, (ii) liquids having low-polarity (e.g., acetone) and high-polarity (e.g., methanol), and (iii) solids having resonant absorption (e.g., lactose monohydrate), broadband absorption (e.g., glass), and high transparency (e.g., polyethylene).

The trainings were focus on THz systems and signal detections. For example, the spectral measurements of glasses with smooth rough and rough surfaces demonstrate that THz wave is less scattered by the rough surface than the infrared wave because of its longer wavelength (Fig.4 (a), (b)). These data strongly evidences that THz wave can be an effective means for the imaging of human skin which is often coarse. As shown in Fig.5, grey body method (warm water in a polyethylene bottle) was applied to characterize three important THz detectors: Golay cell, $LiTaO_3$ pyroelectric detector and THz zero-bias Schottky diode.

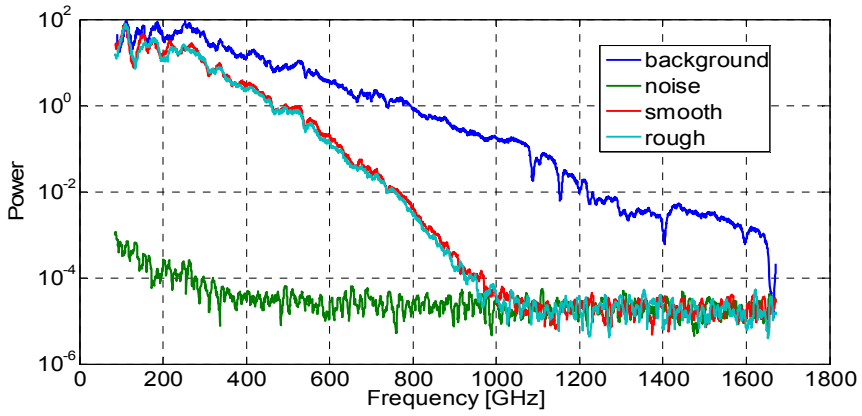

(a)

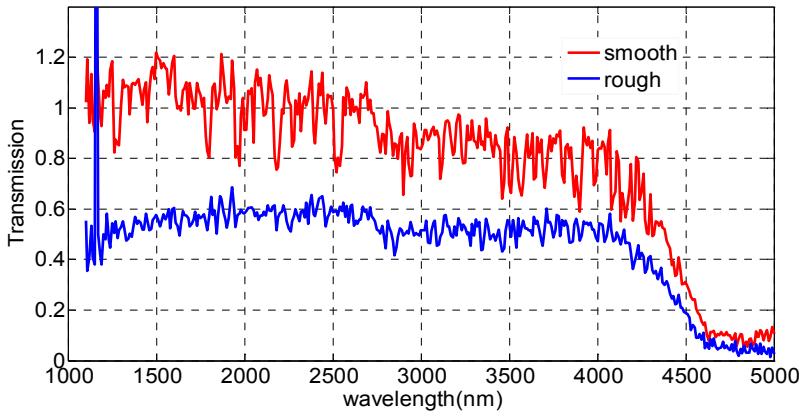

(b)

Figure 4. The transmission spectrums on glasses with smooth and rough surface , measured with PB7100. (a)in the THz range; (b) the mid-infrared range measured with ConerStone 260 ¼ m monochromator.

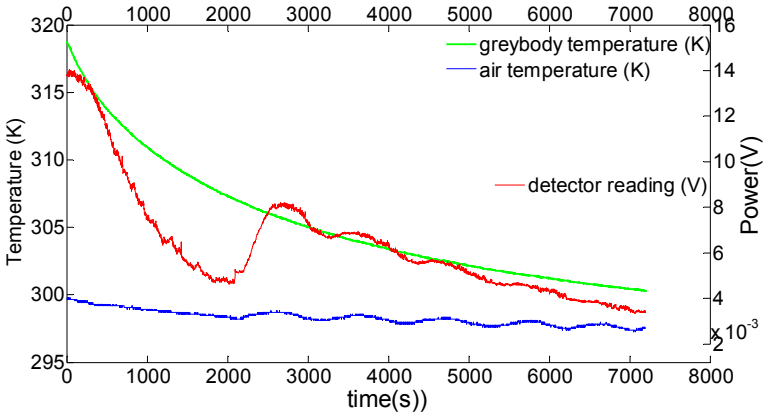

(a)

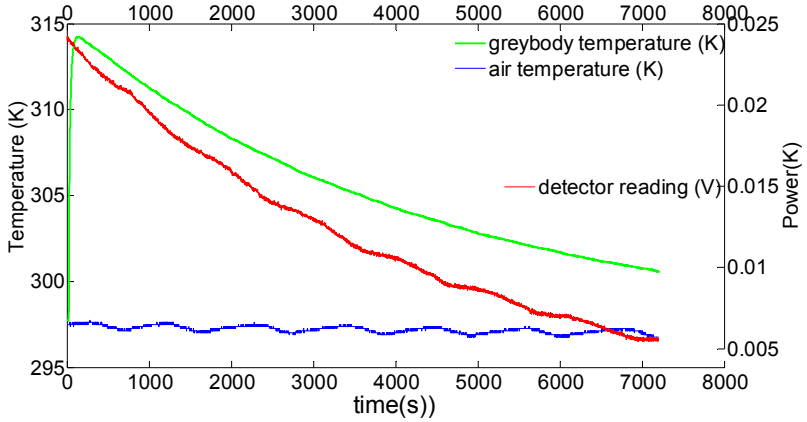

(b)

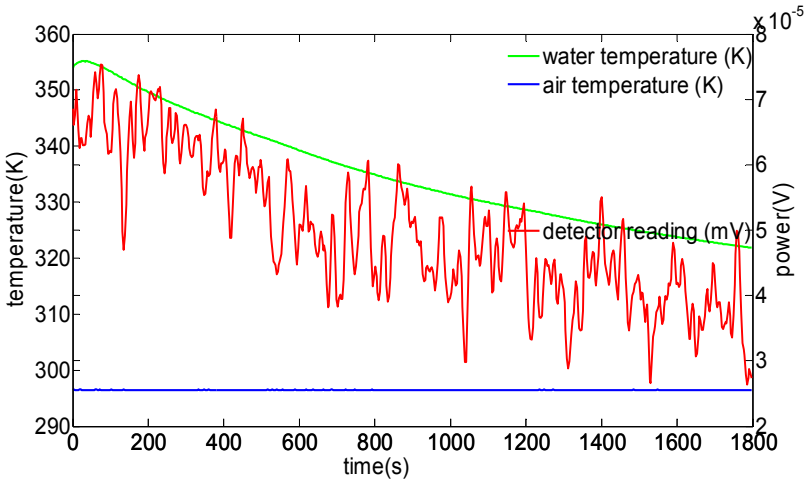

(c)

Figure 5. Greybody characterization of three THz detector categories, (a)Golay cell, (b) pyroelectric and (c) Schottky diode.

V. Experimental Setups for Testing InAs-GaSb THz Lasing Concept

We conduct preliminary studies for engineering implementation of InAs-GaSb THz laser concept with the help of THz training course.

The major device structure we plan to grow and study is illustrated in Fig. 6 (a). The first step is to conduct electroluminescence measurements as shown in Fig 6. (b). These measurements will probe the presence of holes produced by interband Zener tunneling; and the interband tunneling from HH level is such a rapid process that it outpaces the filling-up from optical transition or non-radiative scatterings of electrons which occupy the upper conduction band level. These studies help us decide whether THz light emitting diodes are possible: how much power can be obtained and what is the range of wavelength.

The radiation is inherently TE polarized within this interband InAs/GaSb THz laser. This unique feature allows adapting distributed Bragg reflection (DBR) mirrors for effective mode confinement in the active layer. The vertical-cavity surface emission laser (VCSEL) implementation can be built with dielectric DBRs deposited on the top of n^+ layer and a thin metallic layer on the back of n InAs substrate as illustrated in Fig. 6 (c). The Bragg mirrors consist of multiple periods of dual high/low dielectric layers with very low absorption loss at THz regime (for example, Si/Si_3N_4, Si refractive constant 3.42, Si_3N_4, 1.98). Each layer is with one quarter wavelength of thickness. VCSEL allows a single fundamental mode operation and surface emission. This brings an advantage over quantum cascade laser in which the intersubband emission is intrinsically TM polarized. In that case the metal/dielectric or dual metal waveguide is applied as resonator to confine optical mode, and the output is the edge emission that suffers from poor coupling with the free space due to the small aperture in MBE the material growth direction and the loss from facet reflection. In principle, the TE THz sources we propose can be built into either a large area, high power output single device or a two-dimensional THz laser array on a single chip. The optical aperture can be made large given the freedom to enlarge the horizontal dimensions of device. This perspective is a great advantage for THz spectrum sensing and standoff detection.

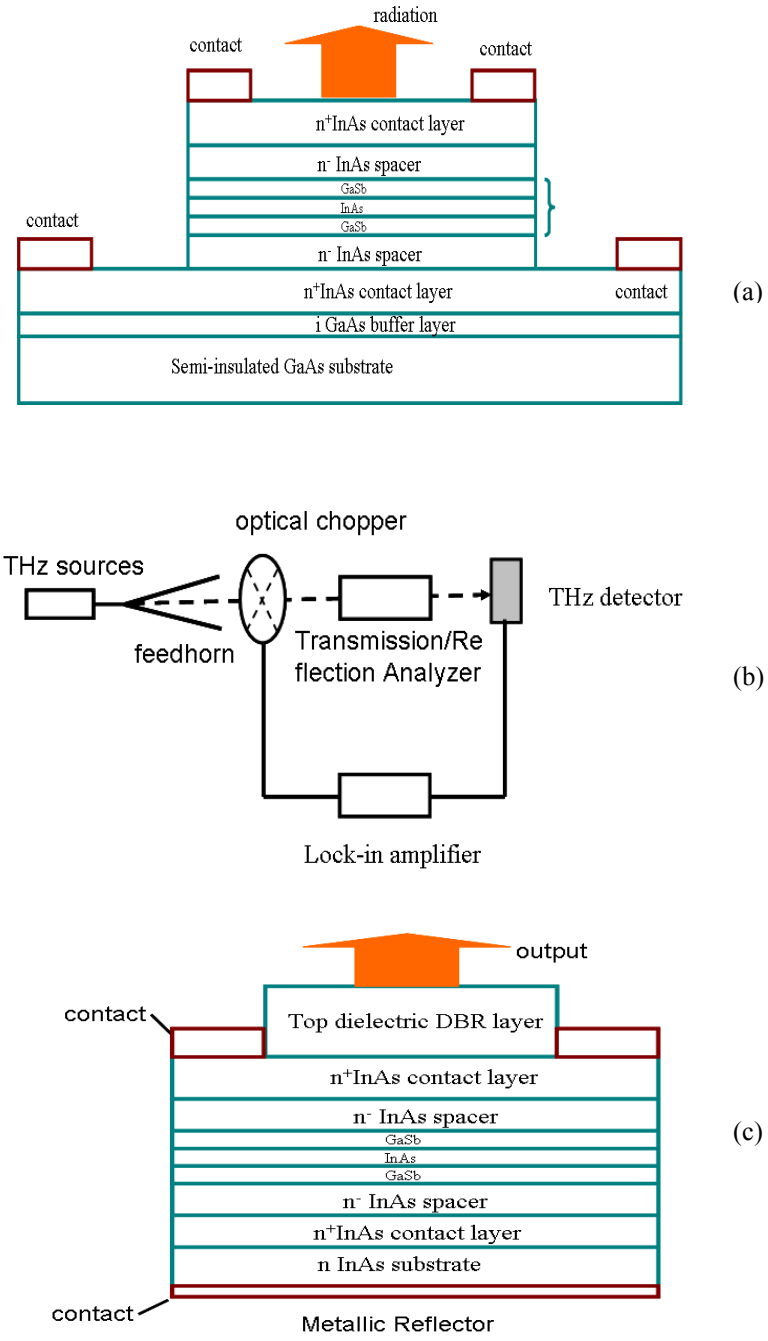

Figure 6. (a) The device structure for electroluminescence measurements. (b) The experimental setup for electroluminescence. (c) VCSEL structure with metallic layer on the bottom.

VI. Modeling and Simulations of Conduction in Molecular Systems

This part work is to develop transport models for designs of functional electronic materials that are based on organic Molecular Switches (OMS). The OMS function material concept is illustrated in Figure 7 (a). When the target agent molecules approach the OMS cells of function material, the energy positions of sensing traps such as Benzoyl Chloride are shift upward or downward arising from the polar twisting due to the interaction between sensing molecules and target molecules (Fig. 7 (b)). This energy-level-switching behavior causes the detectable physical variations on material properties such as conductivity and dielectric constant.

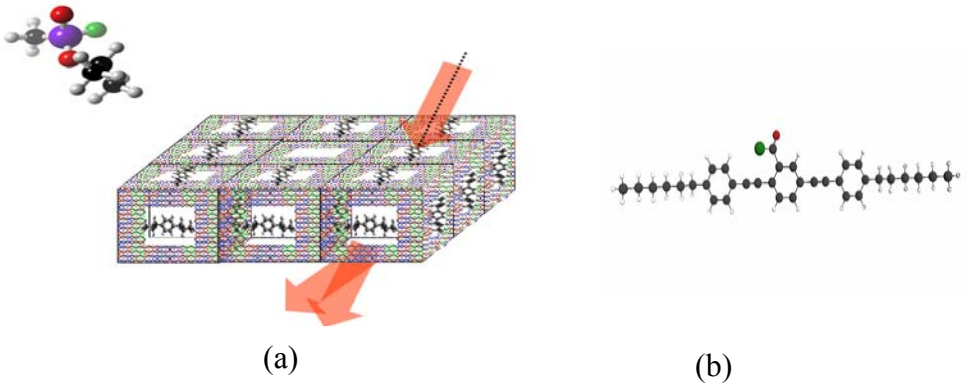

Figure 7. (a) The matrix of OMS. (b) The OMS unit cell with Benzoyl Chloride.

We develop a phenomenological transport model that is traced back to the Marcus theory and Hopfield's work. Both models present actually the same fundamental equation although they were initially developed for different purposes. The Marcus theory is widely applied for the interpretation of chemical reactions while Hopfield's was developed for the photon-assisted charge transfer within bimolecules.

The charge transfer process is illustrated in Fig. 8 (a). The initial site *a* is in the reduced state and the final state *b* is in the oxidized state. The energy states are both broadened into Gaussian distribution due to strong coupling from phonons. The center of Gaussian distribution in the initial reduced state is $E_{o,r} = E_{red} - \lambda$ and the center of Gaussian distribution in the final oxidized state is around $E_{o,r} = E_{red} + \lambda$, where E_{red} is the redox energy that is required to for an electron to be removed from a neutral defect to vacuum. The Franck-Condon rule requires that the positions of nuclei in a molecular entity remain unchanged during electron's transition that is almost instantaneous compared with the slow motion of nuclei. The nuclei's coordinate numbers remains the same during electron's transition. Therefore electron's transfer occurs at the large probability when energy states are in the overlaps of Gaussian distributions between both reduced and oxidized states as shown in Fig. 8 (b). The parabolas are cross each other to keep the same coordinate number in this scenario. In addition, the charge transfer process is accompanied by relaxation of defects through the interaction with its environmental nucleus in which the defect obtains an electron. The equilibrium coordinate is shifted upward or downward in response to the variation on charges carried by the defect nuclei respectively (Fig. 8 (c)).

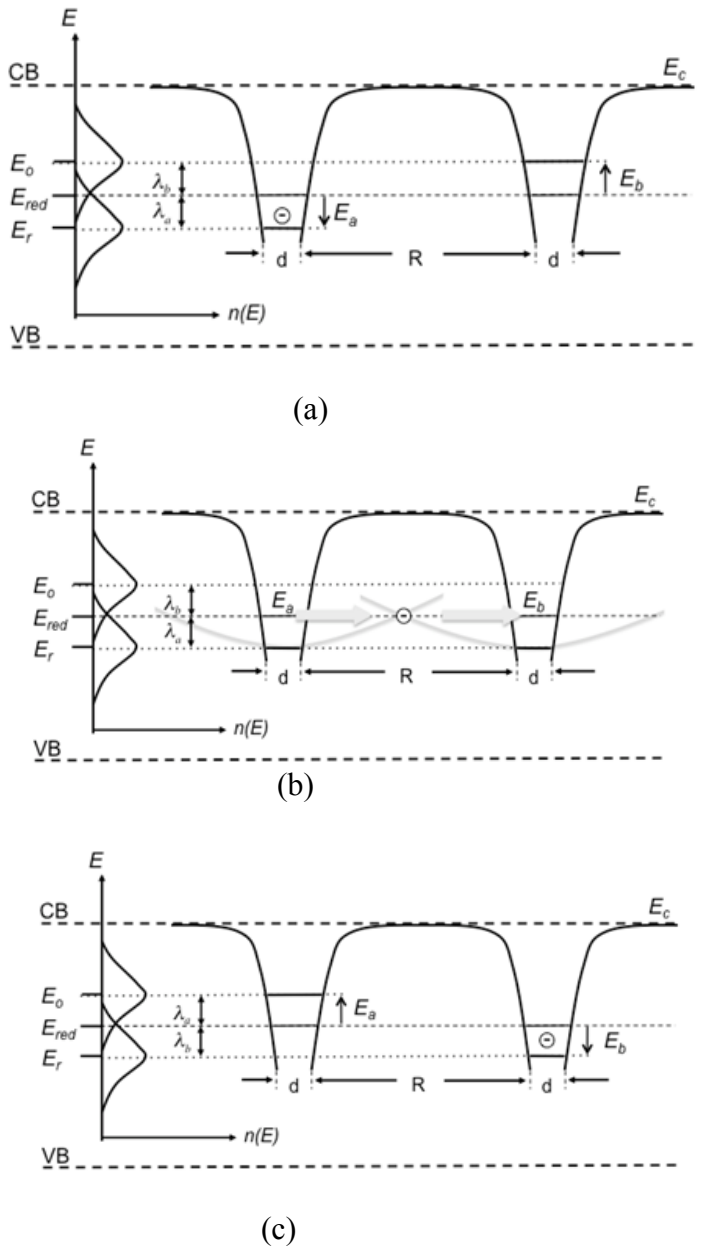

Figure 8. (a) before an electron transfer (b) during electron transfer, and (c) after an electron transfer.

The transition rate between a pair sites in term of the barrier height, site separation, reorganization energy can be evaluated from this physical model. Sequentially, the dc and a.c. and photo-assisted conductivities are evaluated. The numerical calculations plotted in Fig. 9

confirm distinctive on/off switch behavior as the energy position of Benzoyl Chloride is modified by target molecules.

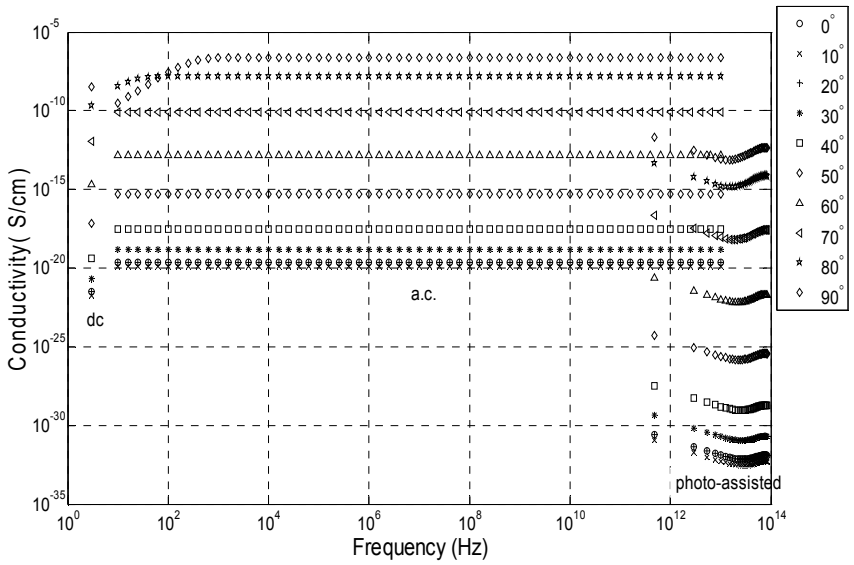

Figure 9. The dc, a..c . and photon-assisted conductivities for OMS based upon Benzoyl Chloride.

VII. Publications and Presentations in 2010-March, 2011

Paper submitted or published in Journals

- Weidong Zhang and Dwight Woolard, "Far-infrared and Terahertz lasing based upon resonant and interband tunneling in InAs/GaSb heterostructure," Applied Physics Letter, vol. 98, 203505, 2011.

- Weidong Zhang and Dwight Woolard, "InAs/GaSb Broken-Gap Heterostructure Laser for Terahertz Spectroscopic Sensing Application", IEEE Transactions on Nanotechnology, Vol. 9, pp.575-581, 2010.

- Weidong Zhang and Dwight Woolard, "A Survey of Recent Patents on THz Radiation Sources", Recent Patents on Electrical Engineering, pp. 193-199, November, 2010.

Paper submitted or published in Conference Proceeding

- Weidong Zhang and Dwight Woolard, "Optical gain in broken-gap nanocrystal arrays for very long wavelength lasing applications": Proceedings: ISSSR conference, Springfield, MO, June 23, 2010.

- Dwight Woolard, Greg Recine, Alexei Bykhovski and Weidong Zhang "Molecular-Level Engineering of THz/IR-Sensitive Materials for Future Biological Sensing Application" Proceedings: SPIE conference 7763 on Terahertz Emitters, Receivers, and Applications (2010).

- Dwight Woolard, Greg Recine, Alexei Bykhovski and Weidong Zhang "Organic and Biological Molecular Switches for Engineering Functional Electronic Materials" Keynote presentation to "Special CMC Symposium on Advanced Materials," International Conference on Computational & Experimental Engineering and Sciences (ICCES), March, 2010.

Conference Presentations

- Dwight Woolard and Weidong Zhang, "THz Lasing Concepts Based upon InAs/GaSb Broken-Gap Heterostructures", International Forum on Terahertz Sepectroscopy and Imaging, Kaiserrslautern, Germany, March 2, 2010.

- Weidong Zhang and Dwight Woolard, "Optical gain in broken-gap nanocrystal arrays for very long wavelength lasing applications", ISSSR Conference, Springfield, MO, June 23, 2010.

Conference Presentations

- Dwight Woolard and Weidong Zhang, " THz Lasing Concepts Based Upon InAs/GaSb Broken-Gap Heterostructures," Photonics West 2011, Terahertz Technology and Applications IV, San Francisco, CA, January 22-27, 2011 (invited talk).
- Weidong Zhang and Dwight Woolard, "An Assessment of Long-Wavelength Optical-Gain in Broken-Gap Heterostrucres and Quantum Dot Arrays," the International Workshop on Optical Terahertz Science and Technology, Santa Barbara, CA, March 13-17, 2011 (poster presentation).